Analytical Methods

Accepted Manuscript

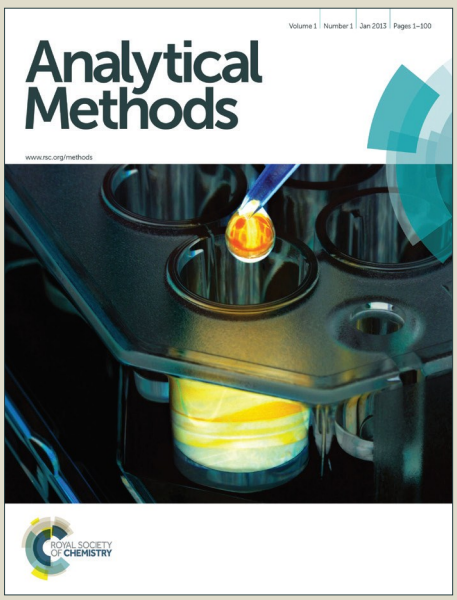

This is an *Accepted Manuscript*, which has been through the Royal Society of Chemistry peer review process and has been accepted for publication.

Accepted Manuscripts are published online shortly after acceptance, before technical editing, formatting and proof reading. Using this free service, authors can make their results available to the community, in citable form, before we publish the edited article. We will replace this *Accepted Manuscript* with the edited and formatted *Advance Article* as soon as it is available.

You can find more information about *Accepted Manuscripts* in the Information for Authors.

Please note that technical editing may introduce minor changes to the text and/or graphics, which may alter content. The journal's standard Terms & Conditions and the Ethical guidelines still apply. In no event shall the Royal Society of Chemistry be held responsible for any errors or omissions in this *Accepted Manuscript* or any consequences arising from the use of any information it contains.

ROYAL SOCIETY OF CHEMISTRY

www.rsc.org/methods

Cite this: DOI: 10.1039/c0xx00000x

www.rsc.org/xxxxxx

ARTICLE TYPE

Gold nanoparticles biofunctionalized (grafted) with chiral amino acid: a practical approach to determining the enantiomeric percentage of the racemic mixtures

Foroogh Keshvari[a], Morteza Bahram*[a] and Amir Abbas Farshid[b]

Received (in XXX, XXX) Xth XXXXXXXXX 20XX, Accepted Xth XXXXXXXXX 20XX
DOI: 10.1039/b000000x

Abstract:

The importance of stereochemistry in chiral drugs is due to the different pharmacological behavior of enantiomers. Enantioseparation methods based on nanoparticles have gained interest recently. The different interaction of enantiomers with chiral nanoparticles encouraged us to determine the enantiomeric percentage of racemic mixtures with modified gold nanoparticles. In this work we applied L-Cysteine capped gold nanoparticles (chiral environment) as a colorimetric sensor for enantio-selective detection of naproxen (NAP) racemic mixtures. The selective and rapid aggregation of modified gold nanoparticles in the presence of R-naproxen allowed us to construct a visual chiral sensor. The results were characterized by TEM, UV-visible, zeta potential and FT-IR measurements. L-Cysteine group functionalized gold nanoparticles (L-Cys-Au NPs) had a cooperative effect on visual inspection of R-naproxen in aqueous solution resulting in sensible changes in color and absorption specifications over S-naproxen. The effect can be monitored with naked eye or using a UV-vis spectrometer. The developed method was utilized for the determination of enantiomeric percentage of the racemic mixtures of NAP in aqueous and plasma samples with satisfactory results. Under optimum conditions, the chiral biosensor exhibited a good linear response to naproxen enantiomers in the range of the concentration from 10 to 200 µM with a limit of detection of 6.02 µM (S/N = 3). Relative standard deviation (R.S.D.) water was 3.8% (n=7).

Keywords: Enantioselective determination, Gold nanoparticles, L-cysteine, chiral sensor, chiral drug

1. Introduction

Chiral drugs exist in a pair of enantiomers. In racemic drugs, single isomer frequently offers different pharmacological activity, biological effect and physiological behavior. Statistics indicates that about half of drugs in use are chiral [1, 2]. It is therefore essential to develop new approaches to determine the

enantiomeric percentage with high efficiency. Many separation-based techniques have already been developed to discriminate the chirality of drugs, including high-performance liquid chromatography (HPLC) [3], liquid chromatography (LC) [4], gas chromatography (GC) [5], capillary electrophoresis (CE) [6], 1H-NMR [7], fluorescence (FL), [8] micellar chromatography [9], and recycling high speed counter-current chromatography (HSCCC) [10]. Chiral selector is the main component in this chiral analysis and interactions between chiral selector and enantiomers results in construction of diastereomeric complexes. Lack of sensitivity, high cost, requiring tedious procedures and time consuming are drawbacks of most of these methods. Therefore, developing simple, fast, cost-effective, high sensitive and high efficiency assay for chiral discrimination is noteworthy.

In order to overcome the above-mentioned problem, the present study demonstrate that the enantiomeric composition of a chiral compound could be determined by utilizing chiral modified gold nanoparticles that lead to different interactions with enantiomers. The different interactions can be monitored by significant changes in surface plasmon resonance (SPR) absorption of gold nanoparticles.

Gold nanoparticles (Au NPs) posses distinguish physical and chemical properties like higher extinction coefficient, excellent biocompatibility and strong surface plasmon resonance (SPR) absorption in the visible wavelength range which depends on their size, shape, interparticle distances, and surrounding medium that make it unique candidate for fabrication of colorimetry chemical and biological sensors [11-14]. High surface-to-volume ratio with excellent biocompatibility for functionalization provided a wide range of innovative colorimetric sensors for detection of metal ions, small molecules, proteins and nucleic acids [15-18]. Up to now, very limited number of chiral discrimination colorimetric sensors has been published using gold nanoparticles. Su et al. have employed N-acetyl-L-cysteine capped gold nanoparticles for colorimetric enantioselective detection and enrichment of L-tyrosine [19]. Recently, Seo et al. have utilized L-proline modified gold nanoparticles and Cu^{2+} ions for determining the enantiomeric excess of histidine [20]. However, to date, the selective interaction of chiral L-cysteine capped Au NPs with drug enantiomers has not been described. In this study, we demonstrate that L-cysteine capped Au NPs can be used as an ultrahigh efficiency enantio discrimination and detection platform for R- and S- naproxen (NAP) racemic mixtures (Fig. 1).

Naproxen is a non-steroidal anti-inflammatory drug (NSAID) and is commonly used for relief of a wide variety of pain, fever, inflammations, and stiffness [21]. (S)-enantiomer is 28-fold more active than the (R)-enantiomer [22]. Over the past decades, many methods for enantioselective determination of naproxen have been delivered such as affinity chromatography [23], spectrofluorometry [24], fluid chromatography [25], and High performance liquid chromatography [26].

L-Cysteine provides chiral environment around Au NPs and cysteine binds to the Au NPs surface via the Au-S covalent bond [27]. Cysteine is sulfur containing nonessential amino acids and has important role in biological systems [28]. The general methods for the cysteine concentration determining include high performance liquid chromatography [29], electrochemistry [30] capillary electrophoresis [31], and mass-spectrometry [32]. A nanoparticle-based strategy was reported to regulate interparticle chiral recognition of enantiomers using enantiomeric cysteines (L and D) and gold nanoparticles as a model system. A key element of this strategy is the creation of a nanoscale environment either favoring or not favoring the preferential configuration of the

pairwise zwitterionic dimerization of the enantiomeric cysteines adsorbed on gold nanoparticles as a footprint for interparticle chiral recognition. This recognition leads to interparticle assembly of the nanoparticles which is determined by the change in the nanoparticles surface plasmonic resonance. While the surface density and functionality of cysteines on gold nanoparticles are independent of chirality, the interparticle chiral recognition is evidenced by the sharp contrast between the interparticle homochiral and heterochiral assembly rates based on a first order kinetic model [33]. L-cysteine plays an important role in the presented method. Chiral structure of L-cysteine provides chiral recognition site on the Au NPs surface and by its interactions with R-naproxen assists the aggregation. Chemical interaction between Chiral L-cysteine on the Au NPs and R-naproxen at the molecular level is the basis of the chiral selectivity in this work. As illustrated in Fig. 2, the possible interactions between L-cysteine and R-naproxen depict a clear molecular-level illustration of the well known three-point contact model for chiral recognition in a simple bimolecular system [34]. The functional groups like hydroxyl, amino and carboxylic acid play important in chiral discrimination role through electrostatic and hydrogen bonding (Fig. 2).

Fig. 3 displays a possible proposed mechanism for the colorimetric detection of R-naproxen. Results determined the spatial orientation of R-naproxen is in more proper direction to interaction than S-naproxen. Probably, the interaction between amino group from the L-cysteine and carbonyl group of naproxen results in forming an imine and later generation of a non-charged oxazolidone cycle [35].

In this work, cysteine-capped Au NPs is introduced as a chiral platform for the rapid colorimetric enantiodiscrimination of naproxen racemic mixtures, as a model system, without any prior derivatization and specific instruments. The results demonstrate that this assay is a simple, rapid, sensitive and reliable colorimetric method for chiral drug recognition in aqueous solutions and plasma samples.

2. Experimental

2.1. Material and Instruments

All chemicals used in the experiments were of analytical grade and were used without further purification. Tetrachloroauric (III) acid trihydrate, trisodium citrate dihydrate, methanol and L-cysteine were obtained from Merck (Darmstadt, Germany). (S) -(+)-naproxen and (R)-(-)-naproxen were purchased from Sigma–Aldrich. The enantiomers stock solution was prepared in methanol and working standard solutions of different enantiomers concentrations were prepared daily by diluting the stock solution with Double distilled water (DDW) .

The UV-visible absorption spectra were monitored at room temperature using Agilent 8453 UV-Visible Spectrophotometer with 1-cm quartz cells.

The size and monodispersity of Au NPs were determined by TEM using transmission electron microscope. The IR spectra were recorded on Thermo-Nicolet Nexus 670 FTIR using KBr pellets.

The Zeta potential values of the dispersions were determined using a Zetasizer Nano ZS apparatus (Malvern Ins., UK).

2.2. Synthesis of gold nanoparticles

The Au seeds were synthesized according to Frens method [36]. Briefly, an aqueous solution of 100 ml of 1 mM $HAuCl_4$ was heated to boiling with stirring; then 10 ml 1% (wt/v)

aqueous sodium citrate was added all at once. The color of the mixed solution changed from yellow to wine red in several minutes, indicating the formation of Au NPs. The boiling and stirring were continued for 15 min. The seed solution was cooled to the room temperature and was stored in a dark bottle at 4°C.

The solution of as-prepared citrate-capped Au NPs is wine red, and has a characteristic LSPR absorption band of Au NPs at 519 nm (λ_{max}) with narrow peak half-width (Fig.4).

2.3. General procedure for colorimetric determination of naproxen enantiomers

The colorimetric detection of aqueous naproxen enantiomers was performed at room temperature. During experiments 1mL of synthesized Au NPs was diluted with 1mL deionized water. 15µL of 0.1mM L-cysteine solution then 300µL of naproxen enantio pure solution or racemic solution and 200µL of 0.05M of NaCl were added to the 2mL of diluted Au NPs solution (final volume 3mL). The UV-visible spectra were obtained during 1 hour (Fig. 5).

3. Results and discussion

3.1. Colorimetric determination of naproxen

The as-prepared Au NPs are stable. The L-cysteine capped Au NPs was selected as chiral matrices to construct a colorimetric chiral biosensor for naproxen enantiomers sensing with the assistance of NaCl. In the presence of R-naproxen, an appreciable red-to-blue color shift of L-cysteine capped Au NPs is observed. However, no color changes were found in the presence of S-naproxen. This selective interaction with one enantiomer, resulting in enantio discrimination in this proposed method. In the presence of R-naproxen, L-cysteine and NaCl, the absorbance at 519 nm reduced and a new absorbance peak at 650 nm in UV-visible absorption spectrum (Fig. 6) is observed. From the Fig. 6 aggregation could be attributed to the binding between R-Naproxen and L-Cysteine capped Au NPs, yielding both a substantial shift in the plasmon band energy to longer wavelength and a red-to-blue color change.

In this work, solutions with different enantiomer percentage of R-naproxen and S-naproxen were prepared and UV-visible spectra of assay solutions were recorded during 60 min. Fig. 7 shows Absorbance changes of the L-cysteine capped AuNP after the addition of various mol fraction of R-naproxen during 60min. Fig.8a shows the absorbance changes in UV-Vis spectra after the addition of various mol fraction of R-naproxen (0.1mM). A color program with increasing mole fraction of R-naproxen is shown in Fig. 8a. The quantitative characteristic of the proposed method based on a linear relationship between A_{650}/A_{519} and mol fraction of R-naproxen is shown in Fig. 8b. The UV-visible spectra of L-Cys capped AuNPs with increasing concentrations using enantiomerically pure R-or S-NAP solution is shown in Fig.9. The absorption intensity at 650 nm gradually increased in the presence of R-NAP (Fig.9A).In sharp contrast to R-NAP, there was no distinct effect on the Au colloids upon the addition of S-NAP.

3.2. Characterization of L-cysteine-capped gold nanoparticles

3.2.1. FT-IR analysis

Fourier transform infrared (FTIR) spectrum is used to identify the possible interactions among L-cysteine capped gold nanoparticles and naproxen enantiomers. The related FTIR spectra are shown in Fig. 10. Fig.10A Shows the FT-IR spectra of gold nanoparticles The main peaks at 3428 cm^{-1}, 1402 cm^{-1} and

1593 cm^{-1} are associated with –OH deformation and C=O stretching of citrate ligands in gold nanoparticles spectra, respectively. Fig.10B Shows the FT-IR spectra of cysteine capped gold nanoparticles. The band at 1593 and 1398 cm^{-1} corresponds to the asymmetric and symmetric stretching of COO^-. A band at 1532 cm^{-1} corresponds to N-H bend and the very broad band of NH_3^+ stretch was observed in the 3000–3500 cm^{-1} range. A band near 2550 cm^{-1} confirms the presence of S-H group in the cysteine molecule. Fig.10C Shows the FT-IR spectra of L-cysteine capped gold nanoparticles in the presence of S-naproxen. The spectra similar to L-cysteine capped gold nanoparticles spectra. Results confirm the lack of an interaction between S-naproxen and L-cysteine capped Au NPs. Fig.2D Shows the FT-IR spectra of L-cysteine capped gold nanoparticles in the presence of R-naproxen. The band at 1708 cm^{-1} corresponds to the stretching of C=N in imine and 1599 and 1399 to the asymmetric and symmetric stretching of COO^-.

3.2.2 Zeta Potential Analysis

The higher zeta-potential value is a key parameter to maintain the stability of suspension because it will make a repulsive force and keep the gold nanoparticles away from each other, which results in a high stability of suspension. In solution, molecules associate with the nanoparticles surfaces and these surfaces bound molecules establish a double layer of charge that prevents nanoparticles aggregation. The surface of the NPs is dynamic and is strongly influenced by the nearby environment. The zeta potential is a measure of the particle's stability. Nanoparticles with zeta potential greater than 20 mV or less than -20 mV have sufficient electrostatic repulsion to remain stable in solution [36]. That the L-cysteine capped nanoparticles are more stable in the absence and presence of S-naproxen is confirmed by the high zeta potential value of -22.7 and -21.2 mV respectively. In contrast, low zeta-potential is seen in the presences of R-naproxen. The zeta potential value was -7.99 mV in the presence of R-naproxen.

3.2.2 TEM analysis

To support the proposed mechanism for the interaction between R-naproxen and L-cysteine modified Au NPs, the morphology of the nanoparticles was evaluated by TEM technique (Fig. 11). The R-naproxen stimulated aggregation of gold nanoparticles was evidenced by TEM images that revealed monodisperse nanoparticles in the absence of S-naproxen and significant aggregation of nanoparticles in the presence of R-naproxen.

3.2. Optimization of the proposed method

3.2.1 Effect of L-cysteine concentration

The effect of L-cysteine concentration was shown in Fig. 12a. The aggregation of Au NPs is attributed to the interaction between R-naproxen and L-cysteine on the surface of Au NPs. The concentration should be as high as possible, but it itself should not induce the aggregation of Au NPs. As the concentration of L-cysteine increased, the absorption value at 650nm went up; indicating the aggregation of Au NPs. 0.5µM of L-cysteine was selected as the optimum value for further experiments.

3.2.2 Effect of pH

The aggregation process was also dependent on the pH of reaction medium. The effect of pH was investigated in the range of 3.0-11.0. The experiment solution pH was 6.7. The pH of solution was adjusted at 3, 5, 9 and 11 by adding HCl (0.1M)

or NaOH (0.1M) solution. When pH was ≤ 5 L-cysteine-Au NPs were unstable and aggregated easily. L-cysteine molecules can form intermolecular hydrogen bonding in acidic medium. The results are shown in Fig. 12b. These results reveal that the rate of aggregation decreases at the higher pH. At the isoelectric point of cysteine (pI=5.02), the -CO_2H groups are mostly deprotonated to –CO_2^- while –NH_2 is protonated to –NH_3^+, maximizing the zwitterionic electrostatic interaction. On the other hand, at higher pH the percentage of –NH_3^+ decreased. Subsequently electrostatic interactions between the –NH_3^+ and the –CO_2^- of L-cysteine are no longer at maximum value. To obtain the maximum response, pH 6.7 was chosen.

3.2.3 Effect of NaCl

The addition of NaCl by decreasing the electrostatic repulsion, promote particles aggregation speed. Fig. 12c showed the absorbance ration of A_{650}/A_{519} in different concentrations of NaCl. As we expected, the aggregation degree of L-cysteine cappd Au NPs increased with the increase of NaCl concentrations and addition of NaCl can make the L-cysteine capped Au NPs more sensitive for R-naproxen determination. Although higher concentrations of NaCl gave better sensitivity, on the other hand Au NPs have aggregated due to excessive NaCl. Au NPs solutions are not stable under high NaCl level. Finally, 1.6mM NaCl was selected as the optimum concentration.

3.2.4 Effect of time

By investigating the effect of time during 60 min, we observed increased in response during the time. In the solutions with more R-naproxen mole fraction there is a dramatic increase in value of A_{650}/A_{519} after 10 min. But in solutions with more S-naproxen the slope is mild. Therefore, we selected 10 min as the optimum time (Fig. 12d).

3.3. Analytical characteristics

Table 1 summarizes the analytical characteristics of the optimized method, including regression equation, linear range, limit of detection and reproducibility.

3.4 Application of the proposed method

The proposed method was applied to the spectrophotometric determination of R-naproxen in racemic mixture in the spiked water samples and human plasma by the proposed method. The results are presented in Table 2. The recoveries are close to 100% and indicate that the proposed method was helpful for colorimetric enantiomer determination. For determination of naproxen in the Human plasma, certain amounts of naproxen were independently spiked into tubes containing 3.0 mL of the plasma. To precipitate the proteins out, the plasma then was mixed with 10 mL of acetonitrile followed by centrifugation at 3,000 rpm for 15 min. The resulted supernatant was used for further analysis under optimum condition. The standard addition method was used in serum samples. Different racemic mixture was spiked to the supernatant. The UV-visible spectra obtained after 10 min.

4. Conclusion

A selective colorimetric R-naproxen sensor was prepared by gold nanoparticles. In the presence of R-Nap, an appreciable red-to-blue color shift of L-cysteine-capped Au NPs

was observed by aggregation of Au NPs. But, no color changes were found in the presence of S-Nap. L-cysteine capped gold NPs as a chiral platform was applied in racemic naproxen. The results indicate that its interaction is enantioselective. This procedure is simple, rapid, selective and sensitive when compared with other methods that have been published for naproxen enantiomer determination.

Notes

*Corresponding author. Tel.: +98 441 2972143; Fax: +98 2776707. *E-mail address:* m.bahram@urmia.ac.ir

[a] *Department of Chemistry,Faculty of Science, Urmia University, Urmia, Iran*

[b] *Department of Pathobiology, Faculty of Veterinary Medicine, Urmia University, Urmia, Iran*

References

1 K.M Rentsch, The importance of stereoselective determination of drugs in the clinical laboratory, J. Biochem. Biophys. Methods. 54 (2002) 1-9.

2 A.J. Hutt, The development of single-isomer molecules: why and how, CNS Spectrums. 7 (2002) 14–22.

3 L. Mosiashvilia, L. Chankvetadzea, T. Farkasb, B. Chankvetadzea, On the effect of basic and acidic additives on the separation of the enantiomers of some basic drugs with polysaccharide-based chiral selectors and polar organic mobile phases, J. Chromatogr. A. 1317 (2013) 167–174.

4 B.K. Hordern, Vishnu V.R. Kondakal, David R. Baker, Enantiomeric analysis of drugs of abuse in wastewater by chiral liquid chromatography coupled with tandem mass spectrometry, J. Chromatogr. A. 1217 (2010) 4575–4586.

5 S. Mohra, J.A. Wei, J. Spreitz, M.G. Schmid, Chiral separation of new cathinone- and amphetamine-related designer drugs by gas chromatography–mass spectrometry using trifluoroacetyl-l-prolyl chloride as chiral derivatization reagent, J. Chromatogr. A. 1269 (2012) 352–359.

6 H. Matsunaga, J. Haginaka, Separation of basic drug enantiomers by capillary electrophoresis using ovoglycoprotein as a chiral selector: comparison of chiral resolution ability of ovoglycoprotein and completely deglycosylated ovoglycoprotein, Electrophoresis 22 (2001) 3251-3256.

7 C. G.M. Hannaa, F.E. Evansb, Optimization of enantiomeric separation for quantitative determination of the chiral drug propranolol by 1H-NMR spectroscopy utilizing a chiral solvating agent, J. Pharm. Biomed. Anal. 24 (2000) 189-196.

8 C.D. Tran, D. Oliveira, Fluorescence determination of enantiomeric composition of pharmaceuticals via use of ionic liquid that serves as both solvent and chiral selector, Anal. Biochem. 356 (2006) 51–58.

9 D. Haupt, C. Pettersson, D. Westerlund, Separation of (R)- and (S)-naproxen using micellar chromatography and an α 1-acid-glycoprotein column: application for chiral monitoring in human liver microsomes by

coupled-column chromatography, J. Biochem. Biophys. Methods. 25 (1992) 273–284.Jana NR, Gearheart L, Murphy C, Jana NR, Gearheart L, Murphy CJ. Chem Commun, J. Chem Commun 7 (2001) 7: 617-618.

10 S. Tonga, Y.X Guana, J. Yanb, B. Zheng, L. Zhaob, Enantiomeric separation of (R, S)-naproxen by recycling high speed counter-current chromatography with hydroxypropyl-β-cyclodextrin as chiral selector, J. Chromatogr. A. 1218 (2011) 5434–5440.

11 M.E. Stewart, C.R. Anderton, L.B. Thompson, J. Maria, S.K. Gray, J.A. Rogers, R.G. Nuzzo, Nanostructured Plasmonic Sensors, Chem. Rev. 108 (2008) 494-521.

12 N.J. Halas, S. Lal, W.S. Chang, S. Link, P. Nordlander, Plasmons in Strongly Coupled Metallic Nanostructures, Chem. Rev. 11 (2011) 3913-3961.

13 P.C. Ray, Size and Shape Dependent Second Order Nonlinear Optical Properties of Nanomaterials and Their Application in Biological and Chemical Sensing, Chem. Rev. 110 (2010) 5332-55365.

14 M.C. Daniel, D. Astruc, Gold Nanoparticles: Assembly, Supramolecular Chemistry, Quantum-Size-Related Properties, and Applications toward Biology, Catalysis, and Nanotechnology, Chem. Rev. 104 (2004) 293-346.

15 Y.J. Kim, R.C. Johnson, J.T. Hupp, Gold Nanoparticle-Based Sensing of "Spectroscopically Silent" Heavy Metal Ions, Nano. Lett. 1 (2001) 165-167.

16 K. Aslan, J.R. Lakowicz, C.D. Geddes, Nanogold plasmon resonance-based glucose sensing. 2. Wavelength-ratiometric resonance light scattering, Anal. Chem. 77 (2005) 2007-2014.

17 H. Wei, B.L. Li, J. Li, E.K. Wang, S.J. Dong, Simple and sensitive aptamer-based colorimetric sensing of protein using unmodified gold nanoparticle probes, Chem. Commun. 36 (2007) 3735-3737.

18 U. Feldkamp, C.M. Niemeyer, Rational design of DNA nanoarchitectures, Angew. Chem. Int. Ed. 45 (2006) 1856-76.

19 H. Su, Q. Zheng, H. Li, Colorimetric detection and separation of chiral tyrosine based on N-acetyl-Lcysteine modified gold nanoparticles, J. Mater. Chem. 22 (2012) 6546-6548.

20 S.H. Seo, S. Kim, M.S. Han. Gold nanoparticle-based colorimetric chiral discrimination of histidine: application to determining the enantiomeric excess of histidine, Anal. Methods. 6 (2014) 73-76.

21 P.A. Todd, S.P. Clissold, Naproxen. A reappraisal of its pharmacology, and therapeutic use in rheumatic diseases and pain states, Drugs 40 (1990) 91–137.

22 I.T. Harrison, B. Lewis, P. Nelson , W. Rooks, A. Roszkowski, A. Tomolonis , J.H. Fried, Nonsteroidal antiinflammatory agents. I. 6-substituted 2-naphthylacetic acids, J. Med. Chem. 13 (1970) 203–205.

23 J.D. Lei, T.W. Tan, Enantioselective separation of naproxen and investigation of affinity chromatography model using molecular imprinting, Biochem. Eng. J. 11 (2002) 175–179.

24 P.C. Damiani, M.D. Borraccetti, A.C. Olivieri, Direct and simultaneous spectrofluorometric determination of

naproxen and salicylate in human serum assisted by chemometric analysis, Anal. Chim. Acta. 471 (2002) 87–96.

25 Y. Yang, B. Su, Q. Yan, Q. Ren. Separation of naproxen enantiomers by supercritical/subcritical fluid chromatography, J. Pharm. Biomed. Anal. 39 (2005) 815–818.

26 D.M. Chena, Q. Fua, N. Lib, S. X. Zhangb, Q.Q. Zhanga, Enantiomeric Separation of Naproxen by High Performance Liquid Chromatography Using CHIRALCEL OD as Stationary Phase, Chin. J. Chem. 35 (2007) 75–78.

27 H. Häkkinen, The gold–sulfur interface at the nanoscale, Nat. Chem. 4 (2012) 443-455.

28 C. Jacob, G.I. Giles, N.M. Giles, H. Sies, Sulfur and selenium: the role of oxidation state in protein structure and function, Angew. Chem. Int. Ed. 42 (2003) 4742–4758.

29 M. Ozyurek, S. Baki, N. Gungor, S.E. Celik, K. Guclu, R. Apak, Determination of biothiols by a novel on-line HPLC-DTNB assay with post-column detection, Anal. Chim. Acta. 750 (2012) 173–181.

30 J.M. Zen, A.S. Kumar, J.C. Chen, Electrocatalytic Oxidation and Sensitive Detection of Cysteine on a Lead Ruthenate Pyrochlore Modified Electrode, Anal. Chem. 73 (2001) 1169–1175.

31 K. Kusmierek, G. Chwatko, R. Glowacki, P. Kubalczyk, E. Bald, Ultraviolet derivatization of low-molecular-mass thiols for high performance liquid hromatography and capillary electrophoresis analysis, J. Chromatogr. B. 879 (2011) 1290–1307.

32 M. Rafii, R. Elango, J.D. House, G. Courtney-Martin, P. Darling, L. Fisher, P.B. Pencharz, Measurement of homocysteine and related metabolites in human plasma and urine by liquid chromatography electrospray tandem mass spectrometry, J. Chromatogr. B. 877 (2009) 3282–3291.

33 I.-I. S. Lim, D. Mott, M. H. Engelhard, Y. Pan, S. Kamodia, J. Luo, P. N. Njoki, S. Zhou, L. Wang and C. J. Zhong, Interparticle Chiral Recognition of Enantiomers: A Nanoparticle-Based Regulation Strategy, Anal. Chem. 81 (2009) 689–698.

34 A. Kuhnle, T.R. Linderoth, B. Hammer, F. Besenbacher, Chiral recognition in dimerization of adsorbed cysteine observed by scanning tunnelling microscopy, Nature 415 (2002) 891–893.

35 E. Sotelo-Gonzalez, M.T. Fernandez-Argüelles, J.M. Costa-Fernandez, A. Sanz-Medel, Mn-doped ZnS quantum dots for the determination of acetone by phosphorescence attenuation, Anal. Chim. Acta. 712 (2012) 120–126.

36 G. Frens, Controlled nucleation for the regulation of the particle size in monodisperse gold suspensions, Nat. Phys. Sci. 241 (1973) 20–22.

37 R. Chandha, S. Bhandari, D. Kataria, S. Gupta, D. S. Jain, Exploring the potential of lecithin/chitosan nanoparticles in enhancement of antihypertensive efficacy of hydrochlorothiazide, J. Microencapsulation 8 (2012) 805–812.

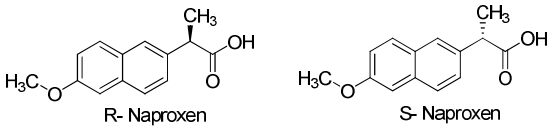

Fig. 1 Chemical structure of naproxen enantiomers

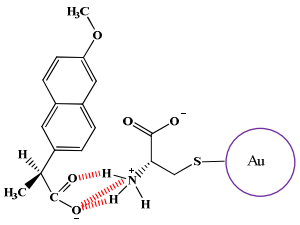

Fig. 2 Proposed interaction of R- naproxen with L-cysteine

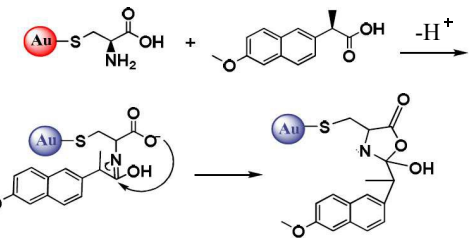

Fig. 3 Scheme of the proposed sensing mechanism

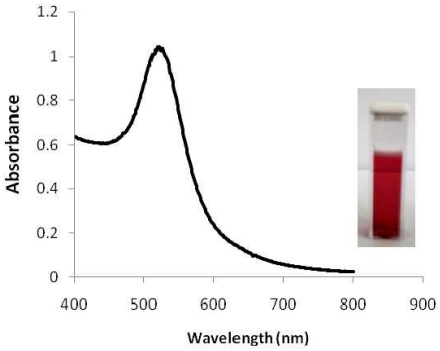

Fig. 4 UV−vis absorption spectra and solution color of citrate-capped Au NPs.

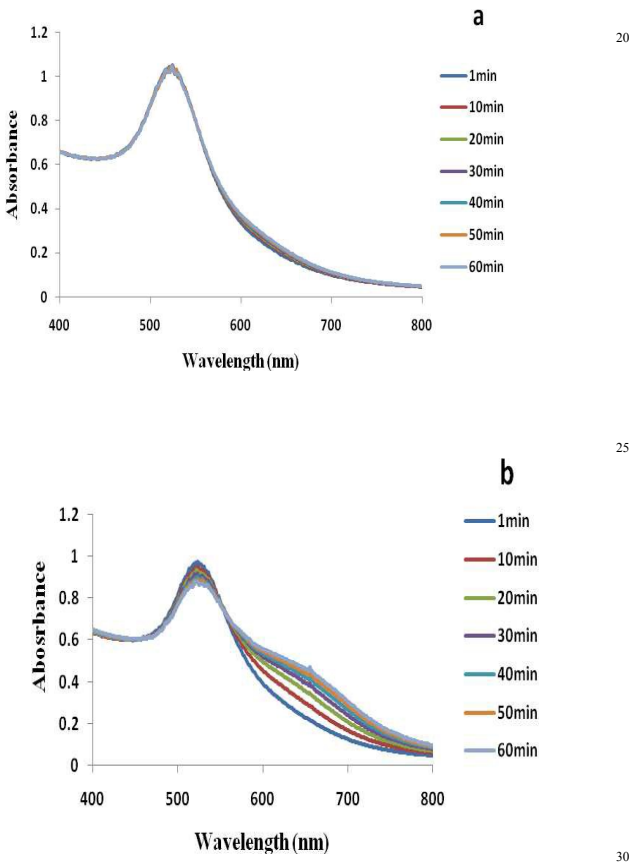

Fig. 5 (a) Time-course study on UV-visible absorbance of L-cysteine capped Au NPs in solution upon addition of (a) 300µL S-naproxen, (b) 300µL R-naproxen in the presence of NaCl

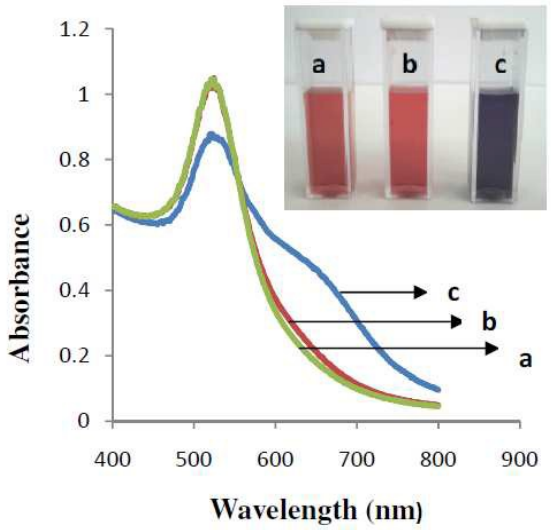

Fig. 6 UV-vis absorption spectra of (a) L-cysteine capped Au NPs (b) L-cysteine capped Au NPs response to S-naproxen (c) L-cysteine capped Au NPs response to R-naproxen

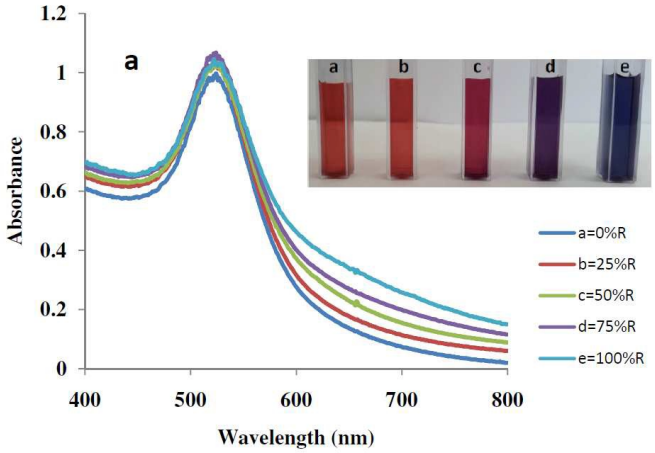

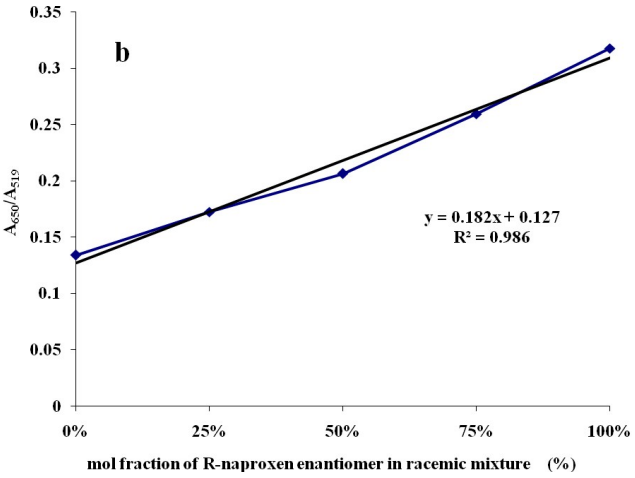

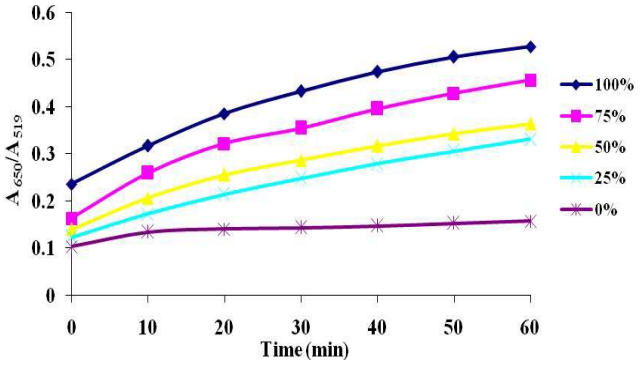

Fig. 7 Absorbance changes of the L-cysteine capped AuNP after the addition of various mol fraction of R-naproxen *versus* time (min)

Fig. 8 (a) The color and UV-vis absorbtion spectra (b) corresponding Plot of A_{650}/A_{519} of racemic solutions containting containing different mol fraction of R-naproxen (time=10min)

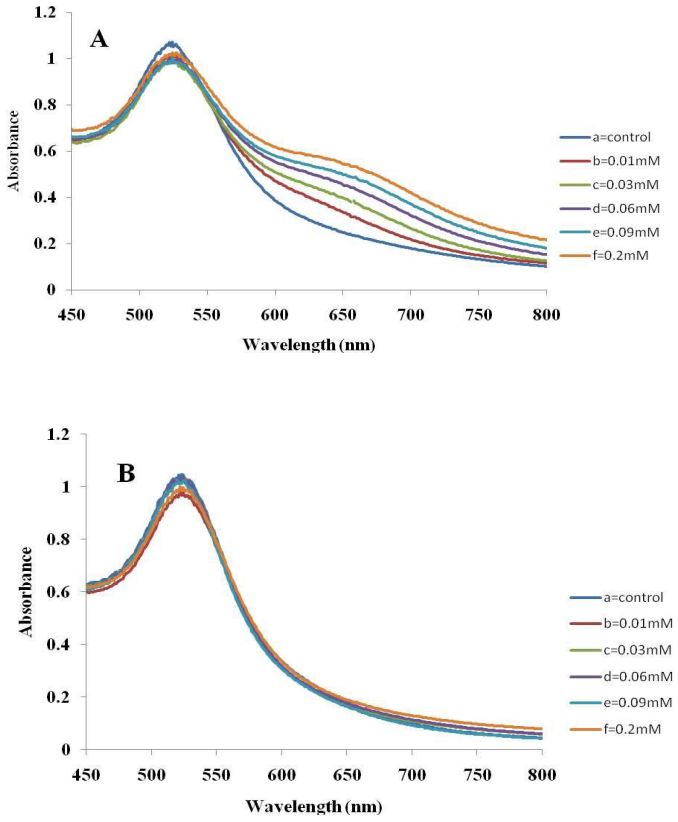

Fig. 9 UV-vis absorption spectra of L-Cys capped Au NPs mixed with R-and S- NAP with increasing concentrations respectively (time=30min)

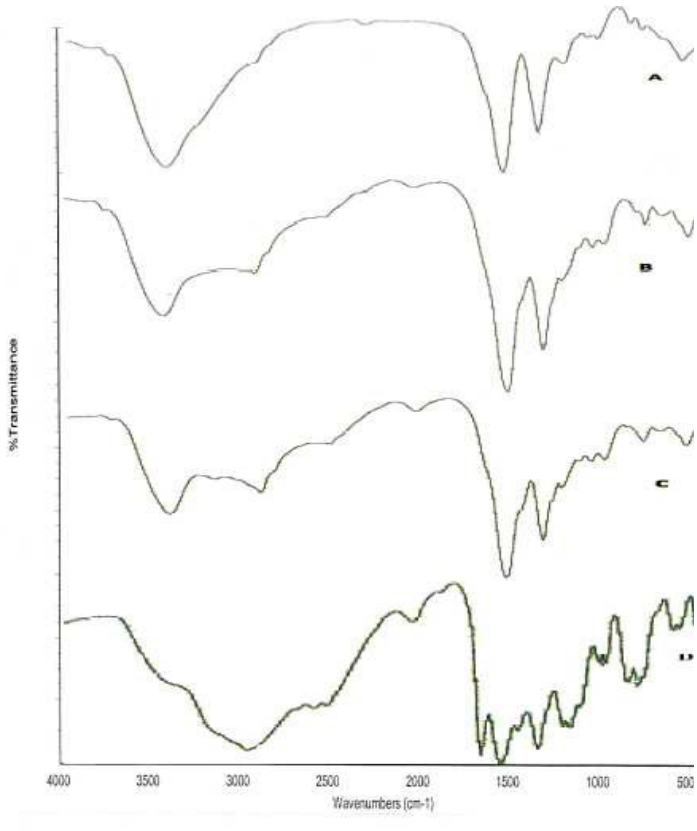

Fig. 10 FT-IR spectra of (A) Au NPs (B) L-Cys capped Au NPs (C) L-Cys capped Au NPs in the presence of S-naproxen (D) L-Cys capped Au NPs in the presence of R-naproxen

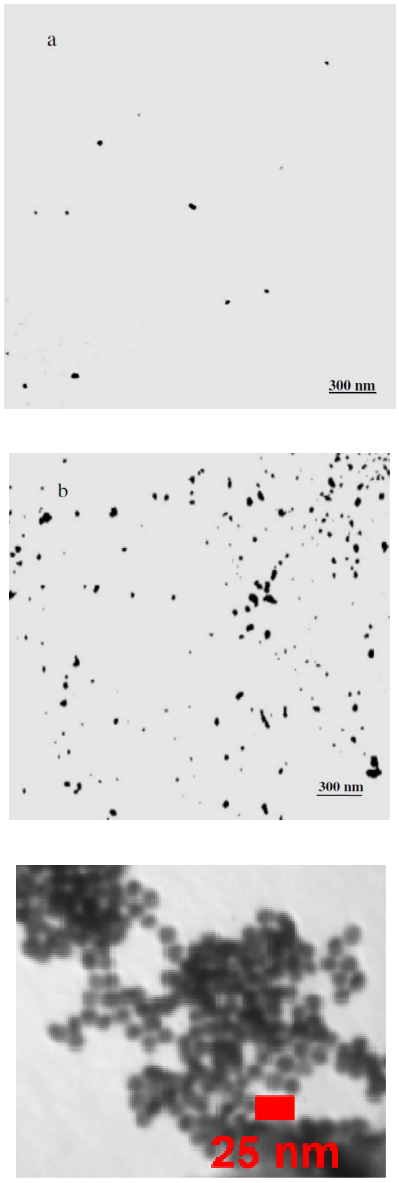

Fig. 11 TEM images of (a) the Au NPs, (b) after addition of cysteine, S-naproxen and NaCl, (c) after addition of cysteine, R-naproxen and NaCl.

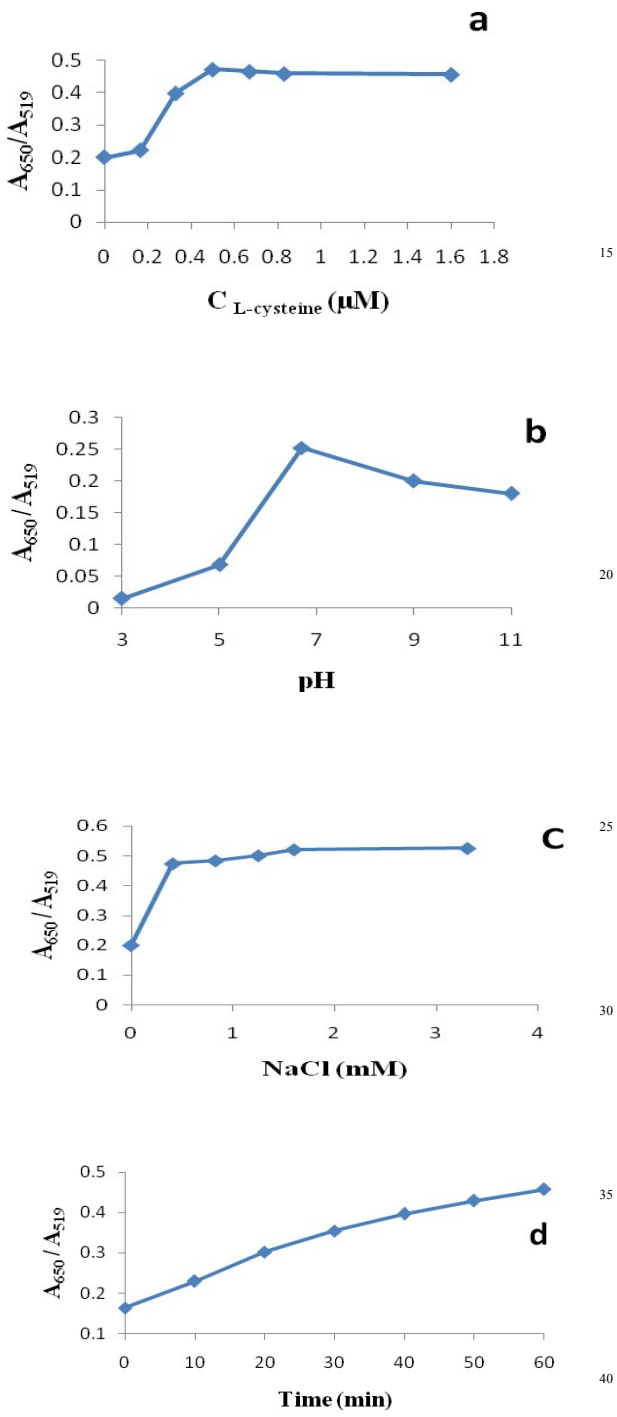

Fig. 12 Effect of different parameters on the response of L-cysteine capped Au NPs to R-naproxen (a) concentration of L-cysteine, (b) pH, (c) concentration of NaCl and (d) Time

Table 1. Analytical characteristics of the proposed method

Regression equation[(a)]	Abs = 3829C +0.025
$R^{2(b)}$	0.997
Linear range (mM)	0.01 – 0.2
LOD (μM) [(c)]	6.02
Repeatability (RSD) [(d)]	3.8
Regression equation for racemic mixture[(e)]	Abs = 0.182X+0.127

(a) Concentration of R-naproxen in mol L^{-1}
(b) Squared regression coefficient.
(c) LOD, limit of detection for S/N = 3.
(d) Relative standard deviation for 7 replicate determination of 0.1 mM R-naproxen.
(e) Mol fraction percentage of R-naproxen in racemic mixture.

Table 2. Enantio determination of R-naproxen in spiked racemic mixture (1,2) and Human plasma (3,4)

Sample	Added (%R)	Added (%S)	Found (%R)	Recovery (%)
Racemic 1	60	40	56	93.3%
Racemic 2	30	70	27.3	91%
Racemic 3	60	40	59	98.3%
Racemic 4	30	70	28.5	95%